



Synthesis, X-ray crystal structures and properties of complex salts and sterically crowded heteroleptic complexes of group 10 metal ions with aromatic sulfonyl dithiocarbimates and triphenylphosphine ligand

Nanhai Singh^{a,*}, Bandana Singh^a, Kamlesh Thapliyal^b, Michael G.B. Drew^c

^a Department of Chemistry, Banaras Hindu University, Varanasi 221 005, UP, India

^b Chemistry Department, IIT Kanpur, Kanpur 208 016, India

^c Department of Chemistry, University of Reading, Whiteknights, Reading RG6 6AD, UK

ARTICLE INFO

Article history:

Received 18 June 2010

Received in revised form 3 July 2010

Accepted 12 July 2010

Available online 25 July 2010

Keywords:

Dithiocarbamate

Complex salts

Heteroleptic

Semi-conductor

Photoluminescence

ABSTRACT

Two new complex salts of the form $(\text{Bu}_4\text{N})_2[\text{Ni}(\text{L})_2]$ (**1**) and $(\text{Ph}_4\text{P})_2[\text{Ni}(\text{L})_2]$ (**2**) and four heteroleptic complexes $\text{cis-M}(\text{PPh}_3)_2(\text{L})$ [$\text{M} = \text{Ni}(\text{II})$ (**3**), $\text{Pd}(\text{II})$ (**4**), $\text{L} = 4\text{-CH}_3\text{OC}_6\text{H}_4\text{SO}_2\text{N}=\text{CS}_2$] and $\text{cis-M}(\text{PPh}_3)_2(\text{L}')$ [$\text{M} = \text{Pd}(\text{II})$ (**5**), $\text{Pt}(\text{II})$ (**6**), $\text{L}' = \text{C}_6\text{H}_5\text{SO}_2\text{N}=\text{CS}_2$] were prepared and characterized by elemental analyses, IR, ^1H , ^{13}C and ^{31}P NMR and UV–Vis spectra, solution and solid phase conductivity measurements and X-ray crystallography. A minor product $\text{trans-Pd}(\text{PPh}_3)_2(\text{SH})_2$, **4a** was also obtained with the synthesis of **4**. The NiS_4 and MP_2S_2 core in the complex salts and heteroleptic complexes are in the distorted square-plane whereas in the trans complex, **4a** the centrosymmetric PdS_2P_2 core is performed square planar. X-ray crystallography revealed the proximity of the ortho phenyl proton of the PPh_3 ligand to $\text{Pd}(\text{II})$ showing rare intramolecular $\text{C-H}\cdots\text{Pd}$ anagostic binding interactions in the palladium cis-5 and trans-4a complexes. The complex salts with σ_{IT} values $\sim 10^{-5} \text{ S cm}^{-1}$ show semi-conductor behaviors. The palladium and platinum complexes show photoluminescence properties in solution at room temperature.

© 2010 Elsevier B.V. All rights reserved.

1. Introduction

Group 10 metal complexes with unsaturated dianionic 1,1- and 1,2-dithioligands where thio functions are present on the same or neighboring carbons have been the main focus of research for the design and study of molecular conductors [1–5]. The higher conductivities of sulfur rich complexes are mainly due to their highly extended delocalized $\text{S}\cdots\text{S}/\text{M}\cdots\text{S}$ intermolecular stacked structures which they exhibit in the solid state. On the other hand, the heteroleptic complexes of platinum(II) with 1,1- or 1,2-dithio ligands containing polypyridyl [6] and less often phosphine ligands [7] have emerged as an interesting class of room temperature solution and fluid state luminescent materials which make them important candidates as photocatalyst in light driven reactions [6]. The incorporation of phosphine ligands into the platinum group metal complexes brings remarkable changes in structural and electronic rearrangements, chemical reactivity and physical properties because of their large steric demands as well as σ -donor and π -acceptor properties.

The dianionic 1,1-dithiocarbamate ligand is akin to the unianionic 1,1-dithiocarbamate (dtc^-) ligand (Scheme 1). Complexes of

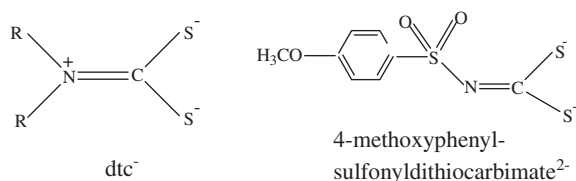
the ligand dithiocarbamate are important because of their resemblance to dithiocarbamate complexes which have been extensively studied and are well known to exhibit a variety of useful applications [8–21].

The three important features associated with the aromatic sulfonyl dithiocarbamate ligands are (i) the delocalization that this ligand can provide beyond M-S_2 bonds through $\text{C}=\text{N}$, C-S and $\text{Ar-SO}_2\text{-N}$ groups (ii) the high electron density presented by the sulfur donors and (iii) the presence of several hard and soft donor atoms N, O and S in the molecule. This makes a significant difference in the structure and properties of their complexes. Thus aromatic sulfonyl dithiocarbimates can be used as important scaffolds for the synthesis of complex salts and heteroleptic complexes. Despite this synthetic versatility [22,23] and the fact that various important properties have been established for the metal complexes that can be formed, scant attention has been paid to this ligand system and only recently the coordination chemistry and some of their applications have been exploited [24–28].

Given these facts we have concentrated our research efforts in this important area and report here the synthesis, crystal structure, molecular electrical conducting and photoluminescent properties of some hitherto uninvestigated complex salts and heteroleptic complexes of nickel(II), palladium(II) and platinum(II) with the ligands dithiocarbamate and triphenylphosphine.

* Corresponding author. Fax: +91 542 2368127.

E-mail addresses: nsingh@bhu.ac.in, nanhai_singh@yahoo.com (N. Singh).



Scheme 1. Structure of ligands.

2. Experimental

2.1. Material and reagents

All reactions were carried out in open atmosphere at ambient temperature. Chemicals were procured from Merck and Sigma Aldrich and used without further purification. The solvents were distilled and dried before use where necessary. Potassium salts of the ligands, L and L', 4-methoxyphenylsulfonyl and phenylsulfonyl dithiocarbamate (4-CH₃OC₆H₄SO₂N=CS₂K₂·2H₂O and C₆H₅SO₂NCS₂K₂·2H₂O) were prepared according to the literature method [29,30] by the reaction of corresponding sulfonamides, potassium hydroxide and carbon disulfide in dimethylformamide and characterized by elemental analyses, IR, ¹H, ¹³C and ³¹P NMR spectra.

2.2. Physical measurements

Experimental details pertaining to the elemental analyses, recording of IR, UV-Vis, photoluminescence and NMR spectra, measurements of solution and pressed pellet conductivity of the complexes are same as described earlier [4,19–21].

2.3. Synthesis

2.3.1. Synthesis of (NBu₄)₂[Ni(L)₂] (**1**)

To a stirring 15 ml aqueous-methanol (2:1) solution of the ligand K₂L·2H₂O (0.750 g, 2 mmol) solid NiCl₂·6H₂O (0.237 g, 1 mmol) was added, followed by 10 ml methanolic solution of NBu₄I (0.738 g, 2 mmol). The reaction mixture was then stirred for 6 h at room temperature. The green color precipitate thus formed was filtered off, washed with the same solvent mixture followed by diethyl ether and dried in vacuo over CaCl₂.

Yield: (0.831 g, 78%), M.P. 122–125 °C. *Anal. Calc.* for C₄₈H₈₆S₆O₆N₄Ni: C, 54.07; H, 8.13; N, 5.25; S, 18.04; Ni, 5.50. Found: C, 53.84; H, 8.10; N, 5.21; S, 17.7; Ni, 5.48%. IR (KBr, cm⁻¹): 1395 ν(C=N), 1262 ν_{asym}(SO₂); 1136 ν_{sym}(SO₂); 940 ν_{asym}(CS₂), 384 ν(Ni-S). ¹H NMR (300.40 MHz, DMSO-*d*₆, ppm): δ 7.66 (d, *J* = 8.79 Hz, 4H, H2 and H6), 6.99 (d, *J* = 8.79 Hz, 4H, H3 and H5), 3.81 (3H, OCH₃); 0.95 (t, 24H, CH₃), 1.37–1.14 (m, 16H, CH₂), 1.63–1.53 (m, 16H, CH₂), 3.81–3.15 (m, 16H, CH₂N), NBu₄⁺. ¹³C (75.45 MHz, DMSO-*d*₆, ppm): δ 209.39 (N=CS₂), 161.78 (C4), 135.85 (C1), 129.44 (C2 and C6), 113.66 (C3 and C5), 55.89 (-OCH₃); 58.08(N-CH₂), 23.57 (CH₂), 19.69 (CH₂), 13.96 (CH₃) NBu₄⁺. UV-Vis (CH₂Cl₂, λ_{max}, nm, ε, M⁻¹ cm⁻¹): 277 (3.47 × 10⁴), 319 (3.70 × 10⁴), 348 (3.45 × 10⁴), 428 (3.94 × 10⁴), 465 (1.14 × 10³) and 610 (94). *A*_M (DMSO (Ω⁻¹ cm² mol⁻¹)): 38.2. σ_{rt} = 4.97 × 10⁻⁵ S cm⁻¹, E_a = 0.56 eV.

2.3.2. Synthesis of (PPh₄)₂[Ni(L)₂] (**2**)

The yellowish green complex **2** was prepared and isolated as described for complex **1** using PPh₄Cl (0.750 g, 2 mmol), NiCl₂·6H₂O (0.237 g, 1 mmol) and the ligand K₂L·2H₂O (0.750 g, 2 mmol).

Yield: (0.945 g, 75%), M.P. 210–212 °C. *Anal. Calc.* for C₆₄H₅₄S₆O₆N₂P₂Ni: C, 61.00; H, 4.32; N, 2.22; S, 15.26; Ni, 4.66. Found: C, 60.51; H, 4.27; N, 2.20; S, 14.81; Ni, 4.61%. IR (KBr, cm⁻¹): 1385 ν(C=N), 1255 ν_{asym}(SO₂); 1140 ν_{sym}(SO₂); 945 ν_{a-}

{sym}(CS₂), 376 ν(Ni-S). ¹H NMR (300.40 MHz, DMSO-*d*₆, ppm): δ 7.98 (d, *J* = 7.2 Hz, 4H, H2 and H6), 6.99 (d, *J* = 8.1 Hz, 4H, H3 and H5), 3.80 (3H, -OCH₃), 7.81–7.62 (m, 40H, PPh₄⁺). ¹³C (75.45 MHz, DMSO-*d*₆, ppm): δ 208.97 (N=CS₂), 161.33 (C4), 135.41 (C1), 129.03 (C2 and C6), 113.23 (C3 and C5), 55.44 (-OCH₃); 135.37 (C4'), 134.65 (C3' and C5'), 130.41 (C2' and C6'), 117.11 (C1') PPh₄⁺. ³¹P {¹H}NMR (121.50 MHz, DMSO-*d*₆): δ 24.32 ppm. UV-Vis (CH₂Cl₂, λ{max}, nm, ε, M⁻¹ cm⁻¹): 273 (3.43 × 10⁴), 309 (3.66 × 10⁴), 322 (3.63 × 10⁴), 355 (3.41 × 10⁴), 430 (3.97 × 10⁴), 477 (0.5 × 10³) and 608 (97). *A*_M (DMSO, Ω⁻¹ cm² mol⁻¹): 36.6. σ_{rt} = 2.55 × 10⁻⁵ S cm⁻¹, E_a = 0.57 eV.

2.3.3. Synthesis of Ni(PPh₃)₂L (**3**)

To a stirred 25 ml methanolic solution of PPh₃ (0.524 g, 2 mmol) was added gradually, 15 ml aqueous-methanolic (1:2) solution of the ligand K₂L·2H₂O (0.375 g, 1 mmol). To this solution, solid NiCl₂·6H₂O (0.237 g, 1 mmol) was added and stirred continuously for 6 h. The peach color solid product thus formed was filtered off and washed with the same solvent mixture followed by diethyl ether and dried in vacuo over CaCl₂.

Yield: (0.692 g, 82%), M.P. 171–173 °C. *Anal. Calc.* for C₄₄H₃₇S₃O₃NP₂Ni: C, 62.63; H, 4.42; N, 1.66; S, 11.38; Ni, 6.87. Found: C, 62.25; H, 4.38; N, 1.64; S, 10.8; Ni, 6.65%. IR (KBr, cm⁻¹): 1410 ν(C=N); 1257 ν_{asym}(SO₂); 1147 ν_{sym}(SO₂); 925 ν_{a-sym}(CS₂) 384 ν(Ni-S). ¹H NMR (300.40 MHz, CDCl₃, ppm): δ 7.76 (d, *J* = 9.00 Hz, 2H, H2 and H6), 6.78 (d, *J* = 8.70 Hz, 2H, H3 and H5), 3.82 (3H, -OCH₃), 7.60–7.16 (m, 30H, PPh₃). ¹³C (75.45 MHz, CDCl₃, ppm): δ 202. (N=CS₂), 161.83 (C4); 133.95 (C1), 128.35 (C2 and C6); 113.16(C3 and C5); 55.40 (-OCH₃); 132.31 (C2' and C6'); 131.89 (C4'), 129.90 (C1'), 128.35 (C3' and C5') PPh₃. ³¹P {¹H}NMR (121.50 MHz, CDCl₃): δ 34.88 ppm. UV-Vis (CH₂Cl₂, λ_{max}, nm, ε, M⁻¹ cm⁻¹): 234 (0.29 × 10⁴); 294 (3.73 × 10⁴), 310 (3.72 × 10⁴), 345 (3.56 × 10⁴), 425 (2.2 × 10⁴), 475 (0.58 × 10⁴) and 597 (50).

2.3.4. Synthesis of Pd(PPh₃)₂L (**4**)

Complex **4** was prepared and isolated as described for complex **3** using K₂PdCl₄ (0.326 g, 1 mmol), PPh₃ (0.524 g, 2 mmol) and K₂L·2H₂O (0.375 g, 1 mmol) and continuously stirred for about 30 h. The yellow solid product isolated was dissolved in CH₂Cl₂:CH₃CN mixture. After one week, from the slow evaporation of the solvent, block shaped crystals of Pd(PPh₃)₂L **4** and needle shaped crystals of Pd(PPh₃)₂(SH)₂ **4a** were obtained.

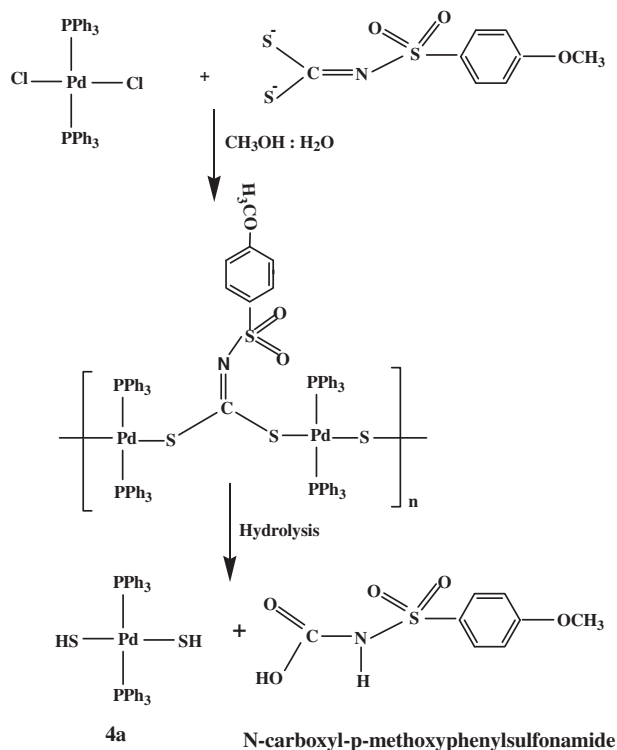
Yield: (0.669 g, 75%), M.P. 205–207 °C. *Anal. Calc.* for C₄₄H₃₇S₃O₃NP₂Pd: C, 59.23; H, 4.18; N, 1.57; S, 10.78. Found: C, 58.82; H, 4.07; N, 1.54; S, 10.24%. IR (KBr, cm⁻¹): 1445 ν(C=N); 1257 ν(SO₂as); 1145 ν(SO₂sym); 922 ν(CS₂), 377 ν(Pd-S). ¹H NMR (300.40 MHz, CDCl₃, ppm): δ 7.83 (d, *J* = 9 Hz, 2H, H2 and H6), 6.8 (d, *J* = 8.7 Hz, 2H, H3 and H5), 7.44–7.19 (m, 30H, PPh₃), 3.83 (3H, -OCH₃). ¹³C (75.45 MHz, CDCl₃, ppm): δ 201.35 (N=CS₂), 161.97 (C4), 135.07 (C1), 129.26 (C2 and C6); 113.12 (C3 and C5); 55.39 (-OCH₃); 134.53 (C2' and C6'), 130.85 (C4'), 129.57 (C1'), 128.47 (C3' and C5') PPh₃. ³¹P {¹H}NMR (121.50 MHz, CDCl₃): δ 31.04 ppm. UV-Vis (CH₂Cl₂, λ_{max}, nm, ε, M⁻¹ cm⁻¹): 273 (3.5 × 10⁴), 307 (3.71 × 10⁴), 364 (3.46 × 10⁴).

2.3.5. Synthesis of Pd(PPh₃)₂(SH)₂ (**4a**)

M.P. 235–240 °C. *Anal. Calc.* for C₃₆H₃₂P₂S₂Pd: C, 62.06; H, 4.63; S, 9.19. Found: C, 61.85; H, 4.60; S, 8.82%. ³¹P {¹H} NMR (121.50 MHz, CDCl₃): δ 24.04 ppm.

2.3.6. Synthesis of Pd(PPh₃)₂L' (**5**)

The yellow complex **5** was prepared and isolated as described for complex **3** using K₂PdCl₄ (0.326 g, 1 mmol), PPh₃ (0.524 g, 2 mmol) and K₂L'·2H₂O (0.346 g, 1 mmol) and continuously stirring the reaction mixture for about 30 h.



Scheme 3. Proposed pathways for the formation of *trans*-4a.

served signals integrate well to the corresponding protons. The ^{13}C NMR signals in the range δ 201.35–209.39 ppm as compared to the potassium salt of the ligands (δ 197–198.5 ppm) are indicative of M–S bonding in the complexes. In the $^{31}\text{P}\{^1\text{H}\}$ NMR spectra of the heteroleptic complexes **3**, **4**, **4a**, **5** and **6**, the singlets at δ 34.88, 31.04, 24.04, 29.87 and δ 17.67 ppm (flanked by the platinum satellites, $^1J(^{195}\text{Pt}-^{31}\text{P}) = 3125$ Hz), respectively, are diagnostic of PPh_3 coordination in magnetically identical environments. Persistence of the rare anagostic intramolecular C–H...M interactions in **4a** and **5** as revealed by X-ray crystallography (vide infra) could

not be confirmed in solution because the anticipated down field shift for the *ortho*-proton of the phenyl ring of the ligand PPh_3 involved in the interactions is not distinguishable as the ligand dithiocarbamate signals also occur in the same region.

3.3. X-ray crystallography

Single crystals of the complexes **1** and **2** were obtained by slow evaporation of $\text{CH}_3\text{OH}:\text{H}_2\text{O}$; those of **3**, **4**, **4a**, **5** and **6** were grown in $\text{CH}_2\text{Cl}_2:\text{CH}_3\text{CN}$ solvent. Crystal data and structure refinement details for **1**, **2**, **4a** and **5** are given in Table 1. ORTEP plots showing the structures of the four complexes are presented in Figs. 1–4, respectively, and selected bond distances and angles are included in Tables 2–4. Complex **1** contains $[\text{NBu}_4]^+$ and **2** contains $[\text{PPh}_4]^+$ cations, both in general positions together with $[\text{Ni}(\text{L})_2]^{2-}$ anions in which the metal atoms are situated on crystallographic centers of symmetry. The immediate square planar geometry around the nickel atom in the complex anion of **1** and **2** (Figs. 1 and 2) is defined by the coordination of four sulfur atoms from the 4-methoxyphenylsulfonamide dithiocarbamate ligand. The Ni(1)–S(1) and Ni(1)–S(2) bond lengths are 2.2057(6), 2.1883(6) Å in **1** and 2.2034(5), 2.2091(5) Å in **2**, respectively. The bite angles S(1)–Ni–S(2), 78.64(2)° and 78.37(2)° in **1** and **2**, respectively, show considerable deviation from the idealized 90° square planar geometry. The atoms Ni, S(1), S(2) and C(2) show very small deviations 0.017, –0.023, –0.023 and 0.028 Å in **1** and 0.031, –0.042, –0.042 and 0.052 Å in **2** from the least-squares plane of the chelate ring. Within the NiS₂C core the Ni–S–C angles are 87.03(7)–87.32(7)° in **1** and 86.96(6)–87.15(6)° in **2** and the S(1)–C(3)–S(2) angles are 106.9(3)° and 107.1(1)° in **1** and **2**, respectively.

The structure of **4a** (Fig. 3) contains discrete *trans*-Pd(PPh_3)₂(SH)₂ molecules. The palladium atom lies on a crystallographic center of symmetry and has a four-coordinate square planar geometry. Pd–S and Pd–P distances are 2.2924(3) and 2.332(2) Å, respectively. The S–Pd–P angles are close to 90°.

In **5** the Pd atom has a four-coordinate square planar environment being bonded to two phosphorus atom of PPh_3 ligands and atoms S(1) and S(2) of the bidentate L' ligand (Fig. 4). The P(1)–Pd–S(1) and P(1)–Pd–S(2) angles are less distorted from the 90° than the P(1)–Pd–P(2) and S(1)–Pd–S(2) angles due to both the ste-

Table 1
Crystallographic data and structure refinement parameters of complexes.

Compound	1	2	4a	5
Empirical formula	$\text{C}_{48}\text{H}_{86}\text{N}_4\text{NiO}_6\text{S}_6$	$\text{C}_{64}\text{H}_{54}\text{N}_2\text{NiO}_6\text{P}_2\text{S}_6$	$\text{C}_{36}\text{H}_{32}\text{P}_2\text{PdS}_2$	$\text{PdC}_{43}\text{H}_{35}\text{P}_2\text{S}_3\text{O}_2\text{N}$
Formula weight	1066.28	1260.10	697.08	862.30
Crystal system	triclinic	triclinic	triclinic	orthorhombic
Space group	<i>P</i> 1	<i>P</i> 1	<i>P</i> 1	<i>Pbca</i>
<i>T</i> (K)	150(2)	150(2)	150(2)	150(2)
Crystal size (mm)	0.30 × 0.05 × 0.05	0.30 × 0.05 × 0.05	0.32 × 0.23 × 0.20	0.34 × 0.29 × 0.25
λ (Å)	0.71073	0.71073	0.71073	0.71073
<i>a</i> (Å)	10.2054(8)	9.0028(8)	9.160(3)	16.4553(15)
<i>b</i> (Å)	11.0022(10)	13.0778(13)	9.668(3)	18.3265(9)
<i>c</i> (Å)	13.5452(11)	13.3095(13)	10.191(4)	25.3452(17)
α (°)	83.689(7)	73.923(9)	73.008(5)	90
β (°)	80.022(7)	88.569(8)	88.240(6)	90
γ (°)	68.105(8)	70.467(9)	67.423(5)	90
<i>V</i> (Å ³), <i>Z</i>	1388.1(2), 1	1415.1(2), 1	793.6(5), 1	7643.3(9), 8
<i>D</i> _{calc} (Mg m ^{−3})	1.276	1.479	1.459	1.952
Reflection collected	7760	7898	5158	27099
Data/restraints/parameter	7760/0/308	7898/0/368	3725/3/188	8689/0/469
Color, habit	needle, green	needle, green	plate, yellow	plate, yellow
<i>F</i> (0 0 0)	574	660	356	4573
μ (mm ^{−1})	0.622	0.677	0.841	1.051
Goodness-of-fit (GOF) on <i>F</i> ²	0.854	1.016	1.146	1.031
Final <i>R</i> indices [<i>I</i> > 2 σ (<i>I</i>)]	<i>R</i> ₁ = 0.0444, <i>wR</i> ₂ = 0.0898	<i>R</i> ₁ = 0.0346, <i>wR</i> ₂ = 0.0881	<i>R</i> ₁ = 0.0664, <i>wR</i> ₂ = 0.1717	<i>R</i> ₁ = 0.0459, <i>wR</i> ₂ = 0.0960
<i>R</i> indices (all data)	<i>R</i> ₁ = 0.0806, <i>wR</i> ₂ = 0.0958	<i>R</i> ₁ = 0.0468, <i>wR</i> ₂ = 0.0910	<i>R</i> ₁ = 0.0940, <i>wR</i> ₂ = 0.2462	<i>R</i> ₁ = 0.0703, <i>wR</i> ₂ = 0.1027
Largest difference peak and hole (e Å ^{−3})	0.510 and −0.525	0.378 and −0.546	1.623 and −2.569	0.551 and −0.733

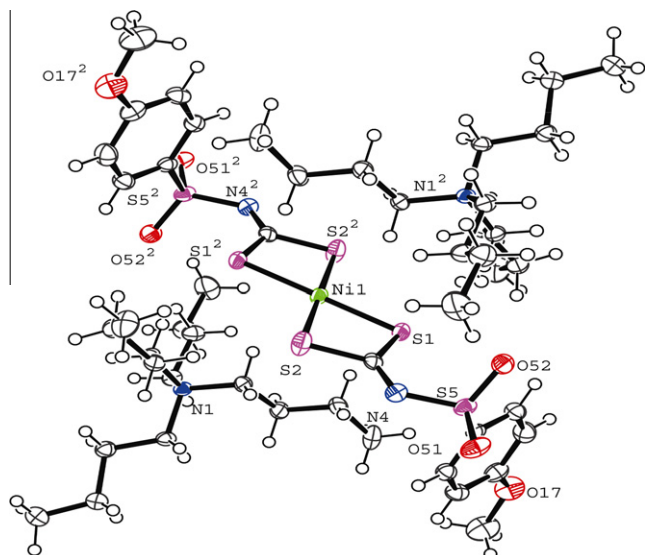


Fig. 1. ORTEP diagram of the $[\text{NiL}_2]^{2-}$ anion and NBU_4^+ cation in **1** with ellipsoids at 50% probability, together with the atom numbering scheme.

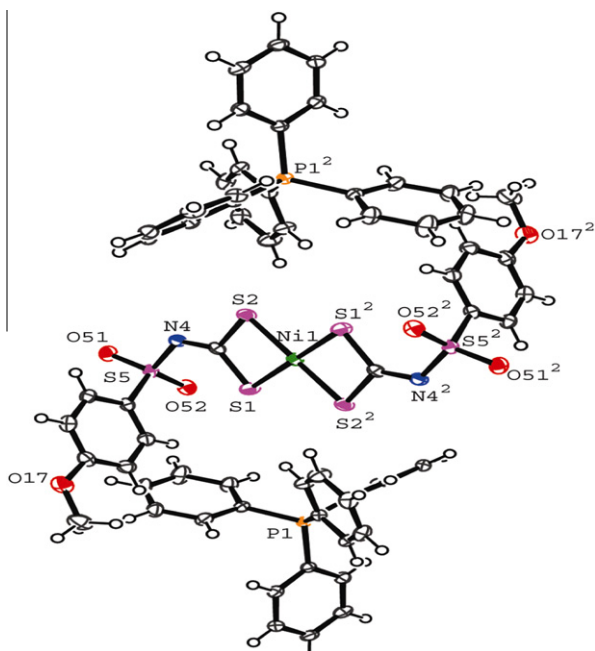


Fig. 2. ORTEP diagram of the $[\text{NiL}_2]^{2-}$ anion and PPh_4^+ cation in **2** with ellipsoids at 50% probability, together with the atom numbering scheme.

ric demands of the PPh_3 ligand and the (S,S) coordination of the ligand dithiocarbamate. The Pd–S(1) and Pd–S(2) bond lengths are 2.3057(9) and 2.3458(9) Å whereas Pd–P(1) and Pd–P(2) Å distances are 2.3134(9) Å and 2.3350(9) Å, respectively.

For **1**, **2** and **5**, the C–S and C=N bond lengths in the range 1.71–1.74 Å and 1.29–1.30 Å show that the carbon–sulfur bonds are considerably shorter than the C–S single bonds (ca. 1.815 Å) due to π -delocalization over CS_2 unit whereas the carbon–nitrogen bonds are reasonably close to C=N double bond in the complexes. Methoxy substitution on the phenylsulfonyl moiety elicits very small changes in the bond dimensions.

The M–S, M–P, C–S and C=N bond lengths in **1**, **2**, **4a** and **5** are well in agreement with the previously reported dimensions for the related dithio complexes [22–28].

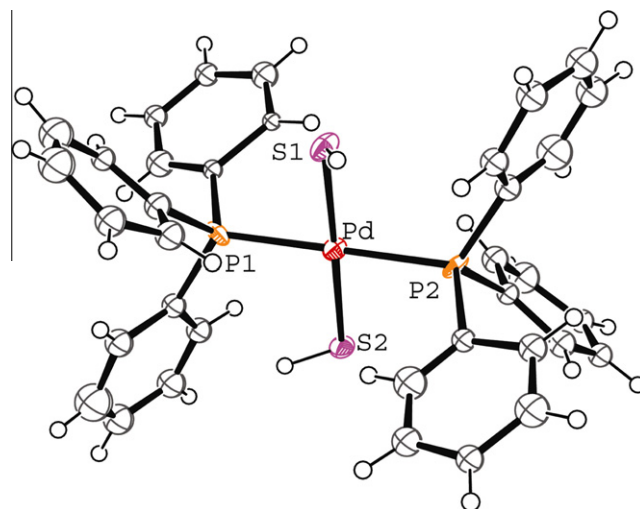


Fig. 3. ORTEP diagram of **4a** with ellipsoid at 50% probability, together with the atom numbering.

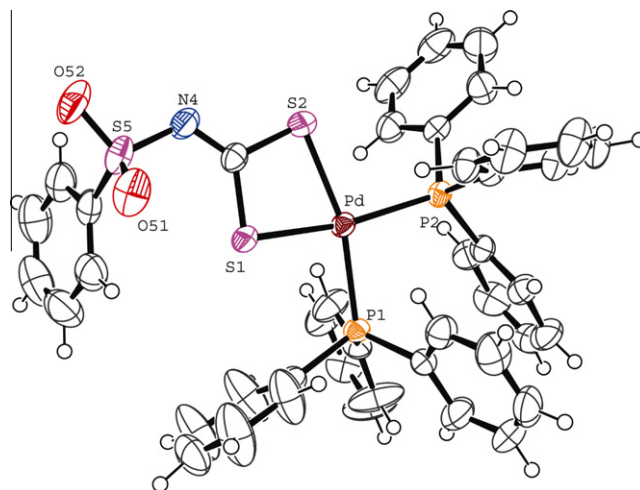


Fig. 4. ORTEP diagram of **5** with ellipsoid at 50% probability, together with the atom numbering.

Table 2
Selected bond length and bond angles of complexes **1** and **2**.

	1	2
<i>Bond length (Å)</i>		
Ni(1)–S(1)	2.2057(6)	2.2034(5)
Ni(1)–S(2)	2.1883(6)	2.2091(5)
S(1)–C(3)	1.728(2)	1.7334(2)
S(2)–C(3)	1.739(2)	1.7341(2)
C(3)–N(4)	1.305(2)	1.306(2)
N(4)–S(5)	1.6213(18)	1.6295(14)
S(5)–O(51)	1.4432(14)	1.4416(12)
S(5)–O(52)	1.4446(15)	1.4379(12)
<i>Bond angles (°)</i>		
S(1)–Ni(1)–S(2)	78.64(2)	78.37(2)
S(1)–C(3)–S(2)	106.87(11)	107.05(9)
C(3)–S(1)–Ni(1)	87.03(7)	87.15(6)
C(3)–S(2)–Ni(1)	87.32(7)	86.96(6)
N(4)–C(3)–S(1)	131.67(16)	132.10(13)
N(4)–C(3)–S(2)	121.45(16)	120.84(13)
O(51)–S(5)–O(52)	116.37(9)	117.11(7)
O(51)–S(5)–N(4)	105.77(9)	105.20(7)
O(52)–S(5)–N(4)	112.49(9)	111.83(7)

Table 3
Selected bond length and bond angles of complex **4a**.

<i>Bond length (Å)</i>	
Pd–S(1)	2.294(7)
Pd–P(1)	2.314(6)
<i>Bond angles (°)</i>	
S(1)–Pd–P(1)	91.85(7)

Table 4
Selected bond length and bond angles of complex **5**.

Pd–S(1)	2.3057(9)	C(3)–S(1)	1.736(4)
Pd–S(2)	2.3498(9)	C(3)–S(2)	1.744(4)
Pd–P(1)	2.3134(9)	S(5)–O(51)	1.429(3)
Pd–P(2)	2.3349(9)	S(5)–O(52)	1.434(3)
C(3)–N(4)	1.297(5)		
<i>Bond angles (°)</i>			
S(1)–Pd–S(2)	75.11(3)	S(2)–Pd–P(2)	95.86(3)
P(1)–Pd–P(2)	98.19(3)	O(51)–S(5)–O(52)	117.6(2)
S(1)–Pd–P(1)	91.39(3)	O(51)–S(5)–N(4)	104.86(19)
S(1)–Pd–P(2)	169.04(3)	O(52)–S(5)–N(4)	111.82(18)
S(2)–Pd–P(1)	165.15(4)		

It is particularly interesting that packing effects together with the steric and electronic impediments of both bulky ligands and diamagnetic square planar Pd(II), d^8 forces the *ortho*-proton on one of the phenyl rings of a PPh_3 ligand to be in close proximity to one of the two vacant axial positions around the metal atom thus creating unusual anagostic or preagostic binding interactions [38–41], and these have been observed in both **4a** C(20)–H(20)···Pd: 2.8 Å; $\angle\text{C–H–Pd}$: 126° and **5** C(25)–H(25)···Pd: 2.7 Å; $\angle\text{C–H–Pd}$: 125°. These interactions are illustrated in Fig. 5 and show that the hydrogen atoms are in approximately axial positions in the metal coordination spheres. The existence of anagostic interactions in solution for these complexes could not be confirmed in the ^1H NMR spectra (*vide supra*). It is worth mentioning that the anagostic and agostic C–H···M interactions are characterized by significantly different structural and spectroscopic characteristics. Anagostic C–H···M interactions are characterized by relatively long M···H distances (~ 2.3 to 2.9 Å) and large C–H···M angles ($\sim 110^\circ$ to 170°) whereas agostic interactions are characterized by relatively short M–H distances (~ 1.8 to 2.3 Å) and C–H···M angles usually in the range ($\sim 90^\circ$ to 140°) [38–41]. Further, the chemical shifts of agostic hydrogen atoms are typically observed at pro-

nounced upfield region as compared to uncoordinated group whereas anagostic hydrogens show remarkably downfield shift of the involved H atoms. These represent unique examples of anagostic interactions in mixed phosphine–dithioligand complexes. These types of interactions are rarely observed but one example has recently been reported [42] in the dithiolate complex $[\{\text{Ni}(\text{L})_2\text{Cu}\}_6]$ [L contains a 4-methylphenyl ring bonded to the dithioligand] involving the phenyl ring proton of the dithioligand.

The large cations in **1** and **2** prevent any stacking of the anions indeed there are no intermolecular S···S distances less than 6 Å. These result in somewhat lower conductivities of the complex salts (*vide infra*) as compared to the extensive conjugation exhibited in the analogous of maleonitriledithiolate (mnt^{2-}) and 1,3-dithiole-2-thione-4,5-dithiolate (dmit^{2-}) complex salts.[1] In **5** the bulky PPh_3 ligands in the coordination sphere also prevent stacking and there is no intermolecular S···S distance less than 7.5 Å.

For compounds **3** and **6** the crystals were of lower quality and the structures could not be refined successfully. However, cell dimensions and preliminary refinements showed that both are isomorphous with **5** crystallizing in the orthorhombic space group *Pbca*. Cell dimensions are $a = 16.354(3)$, $b = 18.381(3)$, $c = 25.287(4)$ Å, $V = 7601(2)$ Å³, $Z = 8$ for **3** and $a = 16.2469(7)$, $b = 18.222(9)$, $c = 25.135(2)$ Å, $V = 7438(6)$ Å³, $Z = 8$ for **6**. No detailed discussion on the geometric data can be presented on the basis of the data collected.

The crystal structures of **1**, **2** and **5** are stabilized by intermolecular hydrogen bond interactions of the type C–H···S, C–H···O and C–H···N in Table S1 and Fig. S1 (see Supplementary material). The packing of the complex anions in **1** and **2** is characterized by one-dimensional sheet-like arrangements separated by sheets of isolated cations NBu_4^+ or PPh_4^+ . In the anions **1** and **2** the non-bonded intra-ligand S(1)···S(2) separations are 2.784(1) and 2.788(1) Å and the inter-ligand S(1)···S(2) distances are 3.399(1), 3.420(1), respectively. The S(1)–C(3)–N(4)–S(5) torsion angles are 4.3(1), 1.1(1)° with S(1)···S(5) distances of 3.293(1), 3.315(1) Å. Similar dimensions in **5** are S(1)···S(2) 2.838(1) Å, S(1)···S(5) 3.357(1) Å with a torsion angle of 5.8(1)°. In all three structures S···S distances are significantly shorter than the sum of the van der Waals radii (ca. 3.60 Å) of sulfur atoms in the molecule indicating substantial nonbonded intramolecular S···S interaction. In the case of **4a**, C–H··· π (Fig. S2 see Supplementary material) and C–H···S intermolecular noncovalent interactions are present and cause a polymeric chain to be formed in the crystal structure.

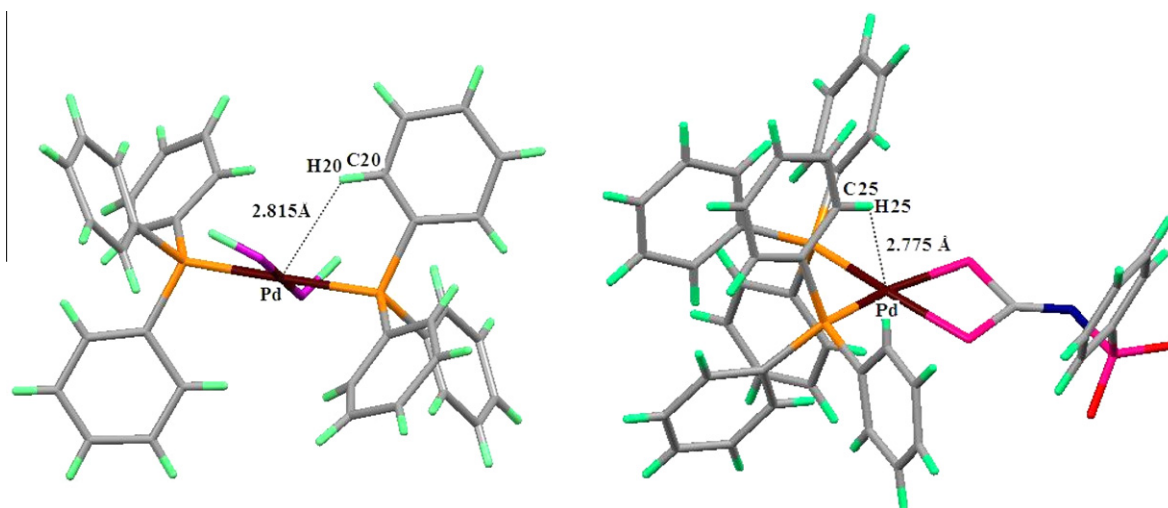


Fig. 5. View of the C–H···Pd anagostic interactions in complex **4a** (left) and **5** (right).

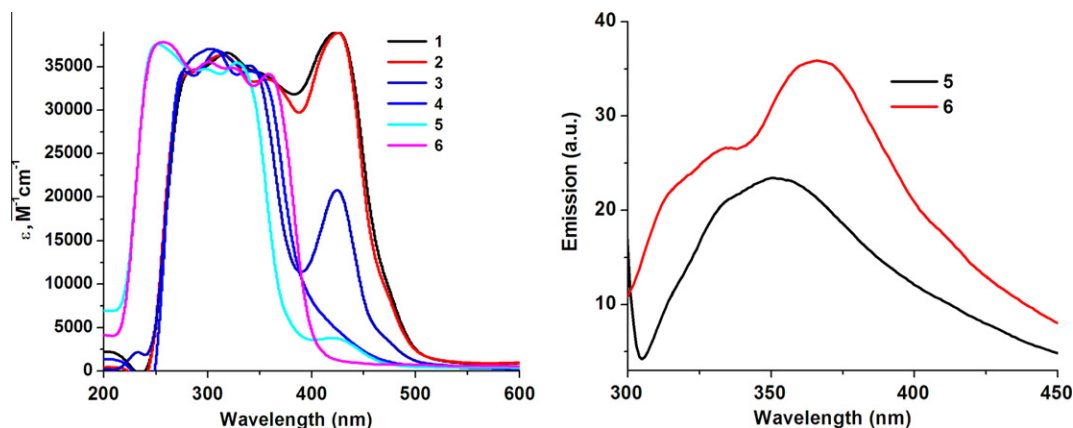


Fig. 6. Electronic absorption (1–6) and emission (5, 6) spectra in CH_2Cl_2 .

3.4. Electronic absorption and emission spectra

The UV–Vis absorption spectra of all complexes obtained in CH_2Cl_2 solution (Fig. 6) and solid in nujol (Fig. S3 in Supporting material) are comparable thereby suggesting that the compounds retain their structure in the solution. In all complexes the absorptions at 234–355 nm are assignable to $\pi-\pi^*$, ILCT transitions. The additional absorptions near 465 and 600 nm in solution as well as nujol mull in the nickel complexes (**1**, **2** and **3**) are assigned to Ni–S, MLCT and d–d transitions for square planar geometry about the metal center [6]. For the heteroleptic palladium and platinum complexes the MLCT and d–d transitions are expected to occur at somewhat higher energies. The absorptions at about 430 nm in **4** and **5** and at 358 in **6** are assigned to MLCT and ILCT [43] transitions, respectively, possibly with some admixture of metal d orbitals.

When excited at 295 nm, **5** shows a photoluminescent emission at ~ 360 nm (Fig. 6) which mainly originates from the $\pi-\pi^*$, ILCT transitions [43]. Upon excitation at 235 nm, **6** displays a photoluminescent emission at ~ 375 nm accompanied with a medium emission band at 325 nm arising from the ILCT transitions [43]. Complexes **1**, **2**, **3** and **4** are non-luminescent because the low spin d^8 , nickel(II) and palladium(II) complexes are well known quenchers [44,45] due to the occurrence of low energy bands in the visible region. It is important to note that the lone pairs of the phosphorus atoms are not involved in π -conjugation to the same extent as the nitrogen lone pairs [44–46]. As a result upon coordination to metal centers phosphine ligands generally do not show larger wavelength shifts in the photoluminescence emission [46].

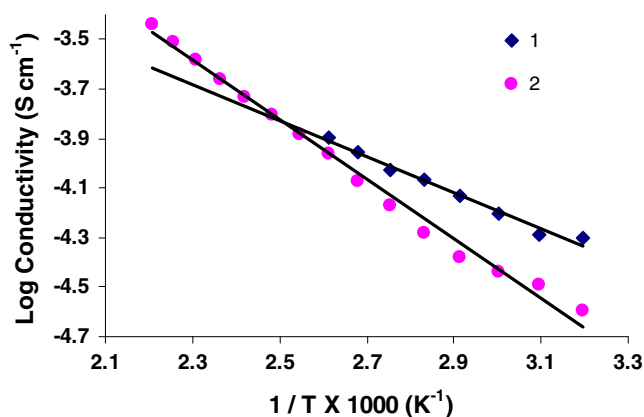


Fig. 7. Temperature dependent electrical conductivities of **1** and **2**.

3.5. Conductivity

Pressed pellet conductivity, $\sigma_{\text{rt}} \sim 10^{-5} \text{ S cm}^{-1}$ of the complex salts **1** and **2** is somewhat low because of absence of $\text{S} \cdots \text{S}/\text{M} \cdots \text{S}$ intermolecular contacts (vide supra in the crystallographic section) which is one of the important prerequisite for the higher conductivities of the complexes (Fig. 7). Despite the variation in the counter cations there is no perceptible enhancement in the conductivity of these salts. Nevertheless, they exhibit semi-conductor behavior as there is progressive increase in the conductivity with increase in temperature which ideally decreases with decreasing temperature in the 313–453 K regions with the band gap of 0.54 eV in **1** and 0.57 eV in **2**. The perceptible enhancement in σ with temperature may be ascribed to the thermal activation of electrons. As expected the heteroleptic complexes **3–6** show insulating behavior due to the presence of bulky PPh_3 ligands which hinder the stacking of the molecules.

4. Conclusions

New complex salts **1** and **2** and sterically congested heteroleptic *cis*-complexes **3**, **4**, **5** and **6** and *trans*-**4a** have been synthesized and fully characterized. The *trans*-complex was obtained as a result of ligand PPh_3 induced catalytic transformation during the course of the preparation of **4**. The presence of rare anagostic $\text{C}-\text{H} \cdots \text{Pd}$ interactions is detected by the single crystal X-ray analyses in **4a** and **5**. The palladium and platinum complexes display photoluminescence properties in solution at room temperature. The low σ_{rt} value $\sim 10^{-5} \text{ S cm}^{-1}$ for **1** and **2** is due to the absence of $\text{S} \cdots \text{S}/\text{M} \cdots \text{S}$ intermolecular contacts which was identified by X-ray crystallography. The complex salts show semi-conductor behavior in the temperature range 313–453 K. The heteroleptic complexes (**3–6**) are insulators.

Acknowledgement

We gratefully acknowledge the Council of Scientific and Industrial Research (CSIR), New Delhi for funding (Project No. 01(2290)/09/EMR-II) and Dr. A. Mishra, for fluorescence spectra. We thank the Department of Chemistry, Banaras Hindu University, EPSRC (UK) and the University of Reading for funds for the X-Calibur CCD diffractometer.

Appendix A. Supplementary material

CCDC 757823, 757824, 772495 and 772496 contain the supplementary crystallographic data for **1**, **2**, **4a** and **5**. These data can be

obtained free of charge from The Cambridge Crystallographic Data Centre via www.ccdc.cam.ac.uk/data_request/cif. Supplementary data associated with this article can be found, in the online version, at doi:10.1016/j.ica.2010.07.065.

References

- [1] P.I. Clemenson, *Coord. Chem. Rev.* 106 (1990) 172.
- [2] P. Cassoux, L. Valade, in: D.W. Bruce, M. O'Hare (Eds.), *Inorganic Materials*, 2nd ed., Wiley, New York, 1996, p. 1.
- [3] A. Kobayashi, E. Fujiwara, H. Kobayashi, *Chem. Rev.* 104 (2004) 5243.
- [4] N. Singh, A. Prasad, R.K. Sinha, *Inorg. Chem. Commun.* 9 (2006) 1058.
- [5] D. Zhu, X.C. Xing, P.J. Wu, P. Wang, D.M. Zhang, D.L. Yang, *Synthetic Met.* 42 (1991) 2541.
- [6] W. Paw, S.D. Cummings, M.A. Mansour, W.B. Connick, D.K. Geiger, R. Eisenberg, *Coord. Chem. Rev.* 171 (1998) 125.
- [7] C.E. Johnson, R. Eisenberg, T.R. Evans, M.S. Burberry, *J. Am. Chem. Soc.* 105 (1983) 1795.
- [8] D. Coucouvanis, *Prog. Inorg. Chem.* 26 (1979) 301.
- [9] G. Hogarth, *Prog. Inorg. Chem.* 53 (2005) 71.
- [10] J. Cookson, P.D. Beer, *Dalton Trans.* (2007) 1459.
- [11] P.J. Heard, *Prog. Inorg. Chem.* 53 (2005) 268.
- [12] E.R.T. Tiekink, I. Haiduc, *Prog. Inorg. Chem.* 54 (2005) 127.
- [13] I. Haiduc, in: F. Devillanova (Ed.), *Handbook of Chalcogen Chemistry*, Royal Society of Chemistry, Cambridge, 2007, p. 593.
- [14] S.J. Lippard, *Pure Appl. Chem.* 59 (1987) 731.
- [15] R. Aragazzi, C.A. Bigozzi, G.M. Hasselman, G.J. Meyer, *Inorg. Chem.* 37 (1998) 4533.
- [16] G. Exarchos, S.D. Robinson, J.W. Steed, *Polyhedron* 20 (2001) 2951.
- [17] G. Exarchos, S.C. Nyburg, S.D. Robinson, *Polyhedron* 17 (1998) 1257.
- [18] L.T. Chan, H.-W. Chen, J.P. Fackler Jr., A.F. Masters, W.-H. Pan, *Inorg. Chem.* 21 (1982) 4291.
- [19] A. Kumar, R. Chauhan, K.C. Molloy, G. Kociok-Kohn, L. Bahadur, N. Singh, *Chem. Eur. J.* 16 (2010) 4307.
- [20] N. Singh, A. Kumar, R. Prasad, K.C. Molloy, M.F. Mahon, *Dalton Trans.* 39 (2010) 2667.
- [21] A. Kumar, H. Mayer-Figge, W.S. Sheldrick, N. Singh, *Eur. J. Inorg. Chem.* (2009) 2720.
- [22] C.J. Burchell, S.M. Aucott, H.L. Milton, A.M.Z. Slawin, J.D. Woollins, *Dalton Trans.* (2004) 369.
- [23] J. Ahmed, K. Itoh, I. Matsuda, F. Ueda, Y. Ishii, J.A. Ibers, *Inorg. Chem.* 16 (1977) 620.
- [24] M.R.L. Oliveira, R. Diniz, V.M. De Bellis, N.G. Fernandes, *Polyhedron* 22 (2003) 1561.
- [25] M.R.L. Oliveira, H.P. Vieira, G.J. Perpetuo, J. Janczak, V.M. De Bellis, *Polyhedron* 21 (2002) 2243.
- [26] S.B. Schougaard, D.R. Greve, T. Geisler, J.C. Petersen, T. Bjornholm, *Synthetic Met.* 86 (1997) 2179.
- [27] R.M. Mariano, H.M. da Costa, M.R.L. Oliveira, M.M.M. Rubinger, L.L.Y. Visconte, *J. Pure Appl. Polym. Sci.* 110 (2008) 1938.
- [28] L.C. Alves, M.M.M. Rubinger, R.H. Lindemann, G.J. Perpetuo, J. Janczak, L.D.L. Miranda, L. Zambolim, M.R.L. Oliveira, *J. Inorg. Biochem.* 103 (2009) 1045.
- [29] K. Hartke, *Arch. Pharm.* 299 (1966) 174.
- [30] H.U. Hummel, U. Korn, *Z. Naturforsch.* 44B (1989) 24.
- [31] G.M. Sheldrick, *Acta Crystallogr.* (2008) 112.
- [32] PLATON: A.L. Spek, *Acta Crystallogr. A* 46 (1990) C31.
- [33] M.N. Burnett, C.K. Johnson, ORTEP-III, Oak Ridge Thermal Ellipsoid Plot Program for Crystal Structure Illustrations, Report ORNL-6895, Oak Ridge National Laboratory, Oak Ridge, TN, USA, 1996.
- [34] H. Kuniyasu, K. Sugoh, M.S. Su, H. Kurosawa, *J. Am. Chem. Soc.* 119 (1997) 4669.
- [35] G. Cavinato, L. Toniolo, *Inorg. Chim. Acta* 52 (1981) 39.
- [36] L. Rigamonti, C. Manassero, M. Rusconi, M. Manassero, A. Pasini, *Dalton Trans.* (2009) 1206.
- [37] W.J. Geary, *Coord. Chem. Rev.* 7 (1971) 81.
- [38] M. Brookhart, M.L.H. Green, G. Parkin, *Proc. Natl. Acad. Sci.* 104 (2007) 6908.
- [39] H.V. Huynh, L.R. Wong, P.S. Ng, *Organometallics* 27 (2008) 2231.
- [40] Y. Zhang, J.C. Lewis, R.G. Bergman, J.A. Ellman, E. Oldfield, *Organometallics* 25 (2006) 3515.
- [41] D. Braga, F. Grepioni, K. Biradha, G.R. Desiraju, *J. Chem. Soc., Dalton Trans.* (1996) 3925.
- [42] R. Angamuthu, I.L. Gelauff, M.A. Siegler, A.L. Spek, E. Bouman, *Chem. Commun.* (2009) 2700.
- [43] S.P. Kaiwar, A. Vodacek, N.V. Blough, R.S. Pilato, *J. Am. Chem. Soc.* 119 (1997) 3311.
- [44] E.G. Bakalbassis, G.A. Katsoulos, C.A. Tsipis, *Inorg. Chem.* 26 (1987) 3151.
- [45] J.-S. Yang, S.-Y. Chiou, K.-L. Liao, *J. Am. Chem. Soc.* 124 (2002) 2518.
- [46] J.R. Lakowicz, *Principles of Fluorescence Spectroscopy*, 3rd ed., Springer, Baltimore, MD, 2006.